Hydrogen Enhanced the Myogenic Differentiation of Adipose Mesenchymal Stem Cells Through P38 MAPK Signaling Pathway

Wenyong Fei
Northern Jiangsu People's Hospital https://orcid.org/0000-0001-7004-7160
Erkai Pang
Dalian medical university
Lei Hou
Dalian medical university
Jihang Dai
Dalian medical university
Mingsheng Liu
Dalian medical university
Xuanqi Wang
Dalian Medical University
Bin Xie
Dalian Medical University
Jingcheng Wang (jingchengwang123@163.com)
Northern Jiangsu people's hospital

Research Article

Keywords: Hydrogen, Myogenic Differentiation, Adipose-derived Mesenchymal Stem Cells, P38 MAPK signaling pathway

Posted Date: November 9th, 2021

DOI: https://doi.org/10.21203/rs.3.rs-1042384/v1

Abstract

Purpose: This study aims to clarify the systems underlying regulation and regulatory roles of hydrogen in the myogenic differentiation of adipose mesenchymal stem cells (ADSCs).

Materials and methods: In this study, ADSCs acted as an in vitro myogenic differentiating mode. First, the Alamar blue Staining and mitochondrial tracer technique were used to verify whether hydrogen could promote cell proliferation. In addition, this study assessed myogenic differentiating markers (e.g., Myogenin, Mhc and Myod protein expressions) based on the Western blotting assay, analysis on cellular morphological characteristics (e.g., Myotube number, length, diameter and maturation index), RT-PCR (Mhc and Myod mRNA expression) and Immunofluorescence analysis (Desmin, Myosin and β-actin protein expression). Lastly, to verify the myogenic differentiating system of hydrogen, Western blotting assay was performed to detect p38 and p-p38 proteins expressions.

Results: Hydrogen can remarkably enhance the proliferation of ADSCs in vitro by increasing the number of single-cell mitochondria and by up-regulating the expression of myogenic biomarkers (e.g., Myod, Mhc and myotube formation). The expressions of both p38 and p-p38 were up-regulated by hydrogen. The differentiating ability was suppressed when the cells were cultivated in combination with SB203580 (p38 MAPK signal pathway inhibitor).

Conclusions: The present study initially indicated that hydrogen can promote myogenic differentiation via the p38 MAPK pathway. Thus, the mentioned results present insights into myogenic differentiation and are likely to generate one potential alternative strategy for skeletal muscle related diseases.

1. Introduction:

Skeletal muscle is commonly impaired for various causes (e.g., trauma and sports activities). The tissue exhibits self-regenerating capability and the inherent satellite cell activity, activating, differentiating and fusing to other satellite cells for forming myotubes with multinucleation [1]. Myotubes have the integration of the existed fibers for the regeneration. Nevertheless, volumetric muscle loss (VML), especially due to tumor removal, degeneration or high-energy trauma, cannot complete the mentioned cascade since fibrosis has more rapid propagation as compared with myogenesis [2, 3]. Muscle degenerating process and volumetric muscle loss currently become conditions causing currently no feasible treating option. Therefore, a novel treatment with fewer complications and satisfactory results are urgently required.

In recent years, researchers have attempted to use the methods of biology and regenerative medicine to promote myogenic differentiation, as they sought to reach the standard of biological healing. To be specific, stem cells in regenerative medicine play an important role in tissue engineering and regeneration because of their excellent regenerative potential, immune regulation and genetic [4, 5]. Based on the above advantages, stem cells are highly expected to promote myogenic differentiation. ADSCs refer to one considerable and effective adult multipotent stem cell source [6], and could be acquired in the body

and act as one source easy to access. In addition, existing study reported [7] differentiating ability exhibited by ADSCs to various lineages including bone [8], cartilage [9], muscle [10] and nerve [11]. Besides, as suggested by ZuK and Mizuno et al., ADSCs could achieve myogenic differentiation. However, studies have shown that only 15% of the stem cells harvested from the processed liposuction (PLA) can fully differentiation [12], and it is difficult for stem cells to return to the injured site after direct transplantation to the target organ, and the cell survival rate is low, and the efficiency of local differentiation is not high [13]. Thus, the clinical myogenic differentiation potential of ADSCs is limited. At present, researchers try to promote myogenic differentiation of stem cells in different ways, such as drug induction, physical induction, cell scaffold induction and so on. Among them, drugs as a more mainstream way of induction, but there are some problems, such as low induction efficiency, obvious inhibition of stem cell self-renewal ability and so on [14]. Therefore, how to make stem cells get efficient myogenic differentiation in the repair area is the main challenge in the treatment of muscle loss.

Hydrogen(H_2), one kind of endogenous gas, was suggested to be one vital energy origin and to critically impact physiologically-related regulating process [15]. Hydrogen molecules can enter tissue as well as performing anti-inflammation-related, antioxidant and anti-apoptotic effects [16]. It is noteworthy that H_2 exhibits great efficacy and safety to cases clinically [17]. For example, Aoki et al found that hydrogen reduced the blood lactic acid level of male football players [18] and improved the decline of muscle function caused by exercise. H_2 can also reduce exercise-induced muscle injury and delayed muscle atrophy, but has no effect on peripheral neutrophil count and neutrophil dynamics and function [19]. In the mouse hindlimb Istroke R injury model, H_2 inhalation significantly reduced the infarct area and tissue structure loss area, alleviated muscle injury, and enhanced functional recovery [20]. However, how H_2 exerts the above effects remains to be further studied.

As indicated from the existing research, ERK1/2, NF-kB, Notch and Wnt signal pathways are capable of regulating the forming and reconstructing processes of general skeletal muscle [21–24]. Moreover, the p38 MAPK class refers to the signal transducing elements that can facilitate the muscle differentiation in vitro, impact the in vivo growth and repair of skeletal muscle, and directly affect the myogenic transcribing elements pertaining to the Myod family [25, 26]. To clarify the action mechanism of H_2, the GEO database was searched, and the H_2-cultured cells were found to be obtained through the high-throughput sequencing of the data set GSE62434. The data were compared with the transcriptional group of normal cultured cells. On the whole, 351 differential genes were obtained by conducting a differential gene analysis. Meantime, as indicated from the analysis of KEGG (Kyoto gene and encyclopedia) enrichment pathway, the differential genes were largely enriched in mitogen-activated protein kinase (MAPK signal pathway) (Fig. 1A,B). Through the further analysis of MAPK signal pathway, we found that the gene differential expression and significance of p38-MAPK signal pathway were the most significant. (Fig. 1C). Besides, according to the results of GSEA enrichment analysis, a significant difference was identified in the expression of p38-MAPK pathway between H_2 culture and normal culture (Fig. 1D,E). As suggested from a GSEA analysis, the function of mitochondria in H_2 culture group was significantly more effective than that in normal culture group (Fig. 1F). As obviously indicated from the mentioned analysis,

p38 MAPK signal pathway and mitochondrial function may impact H_2-induced myogenic differentiation of ADSCs to a certain extent, whereas its specific molecular mechanism remains unclear. For this reason, H_2 was speculated to be capable of regulating the adipose stem cell myogenic differentiation by impacting the p38 MAPK signaling pathway.

The hypothesis of the present study was that H_2 might enhance the myogenic differentiation of adipose mesenchymal stem cells through p38 MAPK signaling pathway. To test this hypothesis, we evaluated the effect of H_2 on myogenic differentiation of adipose stem cells and its molecular mechanism by molecular biology and reverse transcriptase polymerase.

2. Materials And Methods:

2.1 Materials:

Five healthy 2-week-old male rats (From Caavens, Changzhou), adipose stem cells (isolated from primary cells), DMEM medium (Hyclone), 10%Fetal bovine serum (FBS Hyclone), H_2 incubator (PH-A001), 10uM 5-azacytidine (5-Aza)[27], 5uM SB203580 (Beyotime S1863), MTT (Sigma), DMSO (Invitrogen), Alamar blue kit (Solebol A7631), Live-Dead Cell Staining Kit (Biovision K501-100), Mito-tracker (Beyotime C1048), Reverse transcription reagent tool (Thermo #K1622), SYBRGreen PCR kit (Thermo F-415XL), BCA protein assay kit (KGPBCA), Alizarin red staining kit (Solebo G8550), Toluidine blue staining kit (Solebo G3661), Oil red O staining kit (Solebo G1262), β-actin antibody (Proteintech 60008-1-lg), Myosin antibody (Proteintech 60229-l-lg), Desmin antibody (Proteintech 16520-1-AP), Myod (Proteintech), Mhc, p38 (Proteintech), p-p38 (Affinity), GAPDH (Proteintech), Anti-rabbit secondary antibody labeled by CY3 (Proteintech SA00009-2), Anti-mouse secondary antibody labeled by CY3 (Proteintech SA00009-1), Hoechst (Beyotime), CD45 antibody (BD 555485), CD44 antibody (BioLegend 103011), CD90 antibody (BD 555595), CD31 antibody (Abcam ab64543).

2.2 Methods:

2.2.1 Extraction and cultivation of ADSCs

All animal experiments were performed under the approval of the Institutional Animal Care and Use Committee of Jiangsu University. Five two weeks old male SD rats were euthanized with excessive ether asphyxiation. The rats were routinely disinfected by 75% ethyl alcohol, and their blood vessels, fascia and other tissues were removed. The harvested adipose tissue was cut into $1mm^3$ pieces and then placed into a 15 ml centrifuge tube. 0.1% type I collagenase was used to digest tissue for 40-60 min. After filter to remove nondigested tissue, filtrate was collected and seed into tissue culture plastic in culture medium with 10% fetal bovine serum. The incubation was conducted at 37°C with a volume fraction of 5% CO_2, and the liquid was altered after 24 h, 48 h and 72 h. Under the cell concentration of 80%, 0.25% trypsin-EDTA was employed for digestion and subculture. The 3rd generation cells were employed for the immunocytochemical identification and subsequent tests.

2.2.2 Identification of ADSCs

ADSCs were cultured and then identified when 90% of the cells were covered. The cells were digested by trypsin at ambient temperature for 10 min, and it was collected after being centrifuged. Subsequently, the cells were washed with PBS and then prepared into 1*10^^{5}/ml cell number suspension. 100μL of 1*10^^{5} cell suspension was added with 10μL of fluorescently labeled phenotypic antibody (CD45, CD44, CD90 and CD31) respectively for incubation. After the washing process, the expressions of CD45, CD44, CD90 and CD31 surface antigens were detected by performing the flow cytometry.

2.2.3 Identifying process for three-line differentiation of ADSCs

The multilineage differentiating potentials of ADSCs were characterized by osteogenic, adipogenic, and chondrogenic differentiation. Briefly, according to 5*10^4 cells/cm^2 cell density, cells received the collecting and inoculating processes inside the orifice plate. The cells received the culturing process with 5%CO_2 at 37℃. Under the cell confluence of 90%, The cells were cultured in osteogenic, lipogenic and chondrogenic differentiating medium, and identified and analyzed by alizarin red (Solebo G8550), oil red O (Solebo G1262), toluidine blue staining (Solebo G3661). Stained areas were observed under a fluorescence microscope (OLYMPUS, IX71).

2.2.4 Groups and cell proliferation of ADSCs

Cells were collected after being inducted with control, H_2, 5-Aza, H_2+5-Aza for 1, 2 and 3 days. The cell proliferation ability of H_2 and 5-Aza was compared by MTT and Alamar blue staining respectively. Cells were stained with MTT (20μL; 5 mg/ml) for 4 h at 37 ℃. Dimethyl sulfoxide was added to samples and incubated for 30 min at 37 ℃. The absorbance was measured using a microplate reader (Thermo MK3 type) at 492 nM.

Cell samples were taken, and 10μL Alamar blue staining was introduced to 100μL cell suspension at 1- and 3-day induction time. Incubating in an incubator away from light for 6 h, and detecting with microplate reader with a wavelength of 600nm. The diluted AM/PI kit was added and incubated for 30 min before washing. Observed by means of fluorescence microscope (OLYMPUS, IX71). Red and green denote dead cells and live cells, respectively. With ImageJ software (National Institutes of Health, Bethesda), this study determined the fluorescence intensity.

2.2.5 Effect of hydrogen on mitochondria by mito-tracker green fluorescent staining

To investigating the influence exerted by H_2 for mitochondria. First, ADSCs received the inoculating process on confocal petri dishes and the culturing process inside normal medium for 12 h. Next, the cells received the seven-day incubation with control, H_2, 5-Aza, H_2+5-Aza. Then, the medium received the removal and rinsing process by applying PBS, and then it was incubated with the mito-tracker (1:5000-

1:50000) at 37℃ for 15-45 min. Lastly, under a Laster confocal fluorescence microscope, the observation of cells was conducted.

2.2.6 Immunofluorescence detecting process of the expressions of Desmin, Myosin and β-actin in cells

After incubation with control, H_2, 5-Aza, H_2+5-Aza for 7 days, ADSCs were fixed in 4% paraformaldehyde for 15min. Then, 0.1% Triton was used for stabilization at ambient temperature for 15 min. The cells were sealed with 5% FBS for 15 min under the temperature of the ambient. Subsequently, the cells were incubated by using primary antibody at 4℃ throughout the night. After washing, it was incubated at 37℃ for 1h by using secondary antibody. Hochest received the incubating process under ambient temperature and the isolating process away from light for 15min. Lastly, with the use of a fluorescence microscope (OLYMPUS, IX71), the samples were observed.

2.2.7 Real-time PCR analysis of Myod and Mhc

Under the p38 MAPK signal pathway inhibitor (SB203580), the cells were collected after being inducted with control, H_2, 5-Aza, H_2+5-Aza for 7 days. Overall RNA was extracted from the cells under the transfection with the Trizol extraction tool in accordance with the guidelines of the producer. According to the guidelines of the producer, cDNA received the synthesis based on reversely transcribing process with the first strand cDNA synthesis tool. Primers for reverse transcription PCR received the designing and synthesizing processes with Primer Premier 5.0 software (Shanghai Biotechnology, China) based on internal reference of housekeeper gene GAPDH. Table 1 lists primer sequences. After PCR amplification, the results were automatically analyzed by using the fluorescence quantitative PCR tool in the real time, the baseline and threshold were regulated in accordance with the negative control to determine the Ct value of the respective specimen, as well as whether the Ct value was effective based on the fusion curve. For the export, the $2^{-\triangle\triangle CT}$ approach inside gene expressing state differences of control and the concentration groups is: $\triangle$Ct≡ Ct gene-Ct inside. Subsequently the control group $\triangle$Ct remember was obtained for $\triangle$Ct contrast, $\triangle$Ct contrast average was achieved, in which the respective group of $\triangle$Ct minus $\triangle$Ct contrast average, calculated by $\triangle\triangle$Ct value, i.e., the $\triangle\triangle$Ct = $\triangle$Ct sample-$\triangle$Ct contrast, next, the respective group $2^{-\triangle\triangle CT}$ value was calculated, which indicated the comparative expressions of genes.

2.2.8 Observation and analysis of myotube

For investigating the myogenic differentiating system of H_2-induced ADSCs, the authors introduced the SB203580(5uM) to the culture medium (DMEM). Under the p38 MAPK signal pathway inhibitor (SB203580), cells were collected after being inducted with control, H_2, 5-Aza, H_2+5-Aza for 7 days. First, ADSCs received the inoculating process on 24-well plates under a density of 8000 cells /cm for 12 h. Subsequently, the cells received further culturing process with a concentration of H_2, and the medium received the renewal every two days. With the immunofluorescence staining, the myotube formation of ADSCs impacted by hydrogen was determined. ImageJ software was used to obtain the index maturation of myotube (National Institutes of Health, Bethesda, USA).

2.2.9 Western blotting assay

ADSCs were placed in 3.5cm culture dishes with or without SB203580 and cultured with control, H2, 5-Aza and H2+5-Aza for 7 days. Next, cell mass was washed three times with PBS, lysed for 30 min in ice-cold RIPA lysis buffer, and then its protein was quantified. According to the number of samples, the authors introduced the 200 μl BCA working solution (KGPBCA) in samples, and determined the absorbance at 562nm. After being denaturalized, the protein was administrated with polyacrylamide gel and then transferred to the methanol-activated PVDF membrane. After being blocked, the primary antibody was incubated at 4℃ throughout the night: Myod (Proteintech, 1:1000-1: 6000), Mhc (Abcam, 1: 500), p38 (Proteintech, 1: 500-1: 2000), phosphor-p38 (Affinity, 1: 500-1: 2000), GAPDH (Proteintech, 1: 5000). The PVDF membrane was introduced into rabbit secondary antibody or rat secondary antibody (ZSGB-BIO, 1: 5000) solution under the dilution with 1:5000 HRP-labeled solution and was incubated at 37℃ under L h slow oscillation. By employing ECL luminescent solution (Beijing Dingguo ECL-0011), the imprints were developed, and by adopting Image J (NIH, Bethesda, USA), the immunoreaction bands received the quantification.

2.3 Statistical analyses

All experiments were performed in triplicate. For the data recording and the statistical analyses, SPSS 24.0 software in terms of Windows (SPSS Inc., Chicago, IL, USA) was used. The information has the expression to be the mean±standard deviation (SD) pertaining to a range of measuring processes. The authors performed student's t testing process for comparing one individual experiment-related mean with the control mean. $P<0.05$ exhibited statistical significance.

3. Results:

3.1 The evaluation of ADSCs

3.1.1 ADSCs were identified by flow cytometry

ADSCs have no specific surface antigens. Accordingly, the analysis of multiple surface antigens simultaneously to determine the characteristics of adipose stem cells. By flow cytometry, the ADSCs surface markers was tested. We examined the expression of CD31, CD44, CD45 and CD90 in ADSCs at passage 3. Flow cytometry results showed that 1.6% expressed CD31, 95.2% expressed CD44, 1.1% expressed CD45, and 97.4% expressed CD90 (Fig. 1G). CD44 (95.2%) and CD90 (97.4%) express stem cells. The low expressions of CD31 (1.6%) and CD45 (1.1%) excluded epidermal cells and vascular endothelial cells, respectively. For the mentioned results, almost all the experimental cells expressed stem cell characteristics.

3.3.2 ADSCs were identified by three-line differentiation

The multilineage differentiating potentials of ADSCs were characterized through the osteogenic, adipogenic and chondrogenic differentiation. Alizarin red staining under the induction by ADSCs osteogenesis are presented in Fig. 1H(a), demonstrating the appearance of considerable osteoblasts when the induction was achieved. Fig. 1H(b) shows the staining of toluidine blue when the chondroblast induction was achieved, and many chondrocytes were stained. Fig. 1H(c) shows the staining process of oil red O when the lipogenic induction was achieved, and the stained cells were observed as well. In brief, the mentioned cell could achieve a three-line differentiation, which demonstrated that it acts as a rat ADSCs.

3.2 Biocompatibility evaluation of hydrogen

3.2.1 The optimal concentration of hydrogen

Whether H_2 could promote cell viability and proliferation was evaluated by MTT assay (Fig. 2F). After being cultured with H_2 at different concentrations (20%, 50%, 70%), ADSCs showed different cell viability and proliferation. On day 1, no significant difference was fund between the four groups (Control, 20%H_2, 50%H_2, 70%H_2) ($p>0.05$). As compared with other three groups, cells displayed a remarkably high proliferation in 70%H_2 group($p<0.01$) on day 2 and 3. Subsequent experiments were performed at 70% concentration of H_2.

3.2.2 Assessment of cell proliferation by hydrogen

First, we evaluated whether H_2 could promote cell viability and proliferation by MTT and Alamar blue Staining (Fig. 2A-E). In H_2 group, when cultivated for 1 and 3 days, the cells were primarily alive (green), while few had death (red) (Fig. 2A,C). In addition, the cell proliferation characteristic received the quantitative analysis of Live-Dead Cell Staining. As compared with the 5-Aza group, cells displayed a remarkably high proliferation in H_2 group($p<0.01$) on day 1. There was no significant difference between the other three groups (Control, H_2, 5-Aza+H_2) ($p>0.05$). On day 3, compared with 5-Aza and 5-Aza+H_2 groups, H_2 group displayed the highest expression($p<0.01$). Compared with the 5-Aza group, the survival rate of cells in the 5-Aza+H_2 group was still higher($p<0.01$).

Furthermore, the cell proliferation behavior was quantitatively analyzed by Alamar blue assay. On day 1, the cell viability in H_2 group was significantly higher than other groups (5-Aza, 5-Aza+H_2) ($p<0.01$). And, compared with the control group, only the H_2 group showed high proliferation($p<0.05$). Interestingly, compared with the 5-Aza group, the 5-Aza+H_2 group also showed significantly higher proliferation($p<0.01$). On day 3, the cell viability in H_2, 5-Aza and 5-Aza+H_2 groups maintained the same trend as day 1 (Fig. 2B). Based on MTT analysis (Fig. 2D,E), compared with the 5-Aza group, the H_2 group significantly promoted cell proliferation in the first three days($p<0.01$). At the same time, compared to the 5-Aza group, the 5-Aza+H_2 group also increased cell proliferation($p<0.05$). As demonstrated by all the mentioned results, H_2 remarkably enhanced the ADSCs proliferation.

3.2.2 Mito-tracker green fluorescent staining

The green mito-tracker staining was performed for explaining the effect of H_2 on the mitochondria function of ADSCs. (Fig. 2G,H). Obviously, compared with the other three groups, H_2 group expressed significant single-cell mitochondrial fluorescence intensity($p<0.01$). Compared with the control group, the intensity of green fluorescence was significantly decreased in the 5-Aza group($p<0.01$), and the fluorescence expression of single-cell mitochondria was also significantly increased in the 5-Aza+H_2 group compared with the 5-Aza group($p<0.01$).

3.3 Myogenic differentiating effect of hydrogen

3.3.1 Immunofluorescence detecting process of the expressions of Desmin, Myosin and β-actin in cells

To investigate the effect of H_2 on myogenic differentiation at the myoblast stage, ADSCs were employed as an in vitro model of myogenic differentiation. The cells were respectively cultured with 5-Aza, H_2, H_2+5-Aza for 7 days. Fig. 3A shows the results of immunofluorescence staining assay after incubation for 7 days. The immunofluorescence results showed that remarkably higher immunofluorescence expressing states of β-actin and desmin in the H_2 group and 5-Aza group than in the control($p<0.01$). In addition, compared with the control group, the H_2 group showed increased myosin expression($p<0.05$). Additionally, the expressing states of all test antibody were remarkably higher in the H_2+5-Aza group than in the group H_2($p<0.01$). It is noteworthy that the expressing states of the β-actin in 5-Aza and H_2 group were found, whereas noticeable difference was identified between the two groups ($p<0.01$).

3.3.2 Observation and analysis of myotube

Mhc protein immunofluorescence staining assay was performed to visualize the morphology of the formed myotubes in ADSCs. Fig. 3B shows the results of immunofluorescence staining assay after incubation for 7 days. The myotube number, length, diameter and maturation index, were quantified by morphological analysis. Through the determination of the ratio of myotube number with more than 2 nuclei to the total myotube number (myotube maturation index), the myotube maturation was quantified. Compared with control group, 5-Aza+SB203580 and H_{2+}SB203580 groups promoted the high expression of Mhc in the number and length of myotubes($p<0.01$), and there were statistical differences in the diameter and fusion index of myotubes($p<0.05$). It is noteworthy that this study significantly high positive Mhc staining was found in 5-Aza+H2+SB203580 group($p<0.01$). As compared with 5-Aza+SB203580 and H_2+SB203580, 5-Aza+H_2+SB203580 demonstrated the significantly high myotube number, myotube length, myotube diameter and myotube maturation index (Fig. 3B).

3.3.3 Real-time PCR analysis of Myod and Mhc

We further investigated the influence of the H_2 on myogenic genes expression of ADSCs in vitro. Myod and Mhc, the early and late markers of myogenesis, were used to determine the myogenic differentiation

at mRNA level (Fig. 3C). After being cultured for 7 days, the quantitative RT-PCR results showed remarkably higher mRNA expressing states of MyoD and Mhc in the H_2+5-Aza+SB203580 group than other four group($p<0.01$). The Myod and Mhc gene expression of 5-Aza+SB203580 and H_2 +SB203580 was almost the same as control group($p>0.05$). However, compared with the SB203580 group, the expression of MyoD and MHC genes was significantly higher in the H_2 group($p<0.01$). No noticeable difference was identified in Myod and Mhc RNA expressions among the H_2+SB203580 and 5-Aza+SB203580 groups($p>0.05$). As impacted by SB203580, the expressions of Myod and Mhc of the inhibitor groups was also a little less than control group($p<0.01$).

3.3.4 Western blotting assay of Myogenin and Myod

In addition, under the expressing states of Myogenin and Myod (early myogenic marker) and the differentiated myotube marker myosin heavy chain (Mhc), we conducted the western blotting assay for assessing myogenic differentiation (Fig. 4A c-e). As revealed from the results of the western blotting assay, remarkably higher stripe expressing states of Myod, Mhc and Myogenin were found in the H_2 group, 5-Aza group and 5-Aza+H_2 group as compared with those in the control ($p< 0.01$). Besides, the expressing states of Mhc and Myogenin were noticeably higher in the H_2+5-Aza group than those in the H_2 group ($p< 0.01$). It is worth noting that the expressing states of Myod was no noticeable difference was identified in expressing states between the 5-Aza+H_2 group and the H_2 group($p> 0.05$).

3.4 Effect of hydrogen on the phosphorylation of p38 in myogenic differentiation

According to the mentioned results, H_2 could noticeable improve ADSCs proliferation and myogenic differentiation, whereas the molecular system was unclear. Through the analysis of bioinformatics and literature reports, it is known that p38 MAPK was indicated to participate in a range of biological processes of myogenic differentiation. Accordingly, if the phosphorylation levels of p38 MAPK were affected by H_2 regulation in the myogenic differentiation was assessed. ADSCs were incubated in DMEM for 7 days. According to Fig. 4A, the level of p38 and p-p38 phosphorylation in the 5-Aza and H_2 cotreatment group was significantly greater than that in the control ($p<0.01$), which indicated an enhancement in the active form of p38 that promotes differentiation. This result suggests that 5-Aza and H_2 cotreatment during myogenic differentiation could improve p38 activity. It is noteworthy that the levels of p38 and p-p38 in the 5-Aza and H_2 single-treatment groups also significantly increased compared with those in the control, which indicated that either 5-Aza or H_2 treatment during myogenic differentiation increases p38 activity

3.5 The myogenic differentiation facilitated by hydrogen is damaged by the pharmacological inhibition of p38

H_2 regulation improved p-p38 in ADSCs. The mentioned effect, however, was abolished by the presence of specific concentrations of SB203580 (5 nM), a pharmacological inhibitor of p38 that has been

established and applied extensively. In the continued presence of SB203580, rare myotubes were detected based on immunofluorescence staining in the control (Fig. 3B). However, major myotubes with Mhc protein staining received the testing process in H_2, 5-Aza and H_2+5-Aza groups (Fig. 3B). For this reason, this study determined the expressions of proteins and mRNA involved in control, 5-Aza, H_2 and H_2+5-Aza. The quantitative RT-PCR results suggested greater mRNA expressing states of Myod and Mhc in the H_2+5-Aza+SB203580 group than other four groups ($p<0.01$). No noticeable difference was identified in Myod and Mhc RNA expressions in the H_2+SB203580 and 5-Aza+SB203580 groups($p>0.05$). However, both groups were remarkably higher than the SB203580 group ($p<0.05$). As impacted by SB 203580, the expressions of Myod and Mhc of the inhibitor groups were slightly lower than those of the normal group ($p<0.05$) (Fig. 3C). For a broader analysis of the variations in protein, the Western blotting assay was conducted on Myod and Mhc proteins after 7 days of incubation in DMEM with or without SB203580. In addition, as compared with SB203580 and H_2+SB203580 groups, control and H_2 groups had stronger bands, a sharp decline was identified when SB203580 was added. SB203580 groups showed the slight Myod and Mhc protein bands, whereas the rest of the three groups (i.e., H_2+SB203580, 5-Aza+SB203580 and H_2+5-Aza+SB203580) obviously revealed the protein bands. Subsequently, the protein expression of signaling pathway during the myoblast differentiation was detected. There was decline levels of p38 during the introduction of the inhibitor. However, the clear protein band was still found in four groups (i.e., control, H_2+SB203580, 5-Aza+SB203580 and H_2+5-Aza+SB203580). As revealed from the comparison of the four groups, the band of H_2+5-Aza+ SB203580 was the clearest and strongest. The protein bands were similar in expression for H_2+SB203580 and 5-Aza+SB203580, and much clearer and stronger than ADSCs group. For this reason, SB203580 prevents muscle fusion, whereas three group except for SB203580 could still promote myogenic differentiation as impacted by SB203580. In brief, H_2 can activate p38 MAPK signaling pathway by elevating the level of p-p38 protein and facilitate myogenic differentiation of ADSCs.

4. Discussion:

The aim of this study was to investigate the promotive effects of H_2 in proliferation and myogenic differentiation processes of ADSCs as well as the possible signaling pathways involved. H_2 has been proven to be used in multiple biological systems, including those in the Cardiovascular, Digestive and Motor System [28]. In the present study, the H_2 effect can result from the following: 1) reinforcing the single-cell mitochondrial number; 2) stimulating the myogenic biomarking genes' expressing state pertaining to Mhc and Myod, etc.; 3) promoting p38 phosphorylating process inside MAP kinases (MAPK) signaling pathway, by leading the promoted myoblast differentiation.

Over the past few years, uses of H_2 have been largely anticipated as novel medical treatments [29]. H_2 has been employed in different forms to various disease models, and research on its curative effects has progressed rapidly [30, 31]. In the present study, H_2-induced ADSCs were confirmed to exhibit a high biocompatibility in vitro based on MTT and Live-Dead Cell Staining (Fig. 2). It is noteworthy that H_2 can

still alleviate the cytotoxicity of 5-Aza, thereby enhancing the cell viability. Accordingly, H_2 can be significantly ensured to promote the myogenic differentiation of ADSCs. Mitochondria, one of the vital intracellular organelles, significantly impacts various biological processes of eukaryotic cells (e.g., energy generation, calcium balance, intracellular substance metabolism, reactive oxygen production, cell signal transduction and apoptosis] [32–34]. As indicated from the recent advances, adequate mitochondrial function in stem cells is essential to maintain proliferation and differentiation abilities [35, 36]. Accordingly, green mito-tracker staining was adopted to explain the effect of H_2 on the mitochondria of ADSCs. The fluorescence intensity of single cell mitochondria significantly increased after H_2 induction. For this reason, the promoted proliferation of ADSCs was probably because H_2 could increase the mitochondrial number.

Myod and Mhc, the early and late markers of myogenesis [37, 38], were used to determine the myogenic differentiation at mRNA, protein and myotube formation. In the present study, levels of Myod and Mhc both increased significantly when H_2 induction. Notably, H_2 and 5-Aza can synergistically promote the myogenic differentiation of ADSCs. In ADSCs was evaluated using desmin immunofluorescence. Desmin, a muscle-specific member of the family of intermediate filaments, is one of the earliest appearing myogenic markers in both skeletal and heart muscles [39]. Our immunofluorescence results showed that Desmin was significantly overexpressed in H_2-induced ADSCs. Interestingly, in myotubule observation, H_2 and 5-Aza still promoted myotubule maturation under the continuous action of SB203580(Fig. 3B). Therefore, this result indicates that the first is that 5-Aza and H_2 can compete with the p38 MAPK signaling pathway to promote myobgenic differentiation. The second is that H_2 promotes myogenic differentiation via the p38 MAPK signaling pathway, but not only via the p38 MAPK signaling pathway (Fig. 3B). It has been reported that the myogenic differentiation and myoblast's myotube formation noticeably relied upon cell proliferation [40]. The balance between myoblast proliferation and differentiation is important during muscle development [41]. In the present study, the results of the above cell proliferation and myogenic differentiation show a certain correlation. The process of myogenic differentiation into myotube formation is often accompanied by changes in mitochondrial energy metabolism and ROS production. Previous studies have shown that Reactive oxygen species (ROS) is essential mediators of muscle differentiation [42], and it has long been associated with skeletal muscle physiology [43, 44]. However, with the accumulation of ROS, due to its strong oxidation, it can cause irreversible damage to proteins, nucleic acids, sugars, lipids, etc., which significantly inhibits cell activity and leads to cell apoptosis [45, 46]. In the process of myogenic differentiation of stem cells, intracellular ROS level is significantly increased, and the expression of apoptotic proteins such as p53 and other genes is also significantly increased, and cell activity is significantly inhibited [47, 48].

Previous studies have shown that H_2 can reduce ROS level in radiation-injured mice, reduce liver damage, and inhibit radiation-induced apoptosis, thus proving that H_2 can play a protective role on radiation-induced immune system injury by eliminating ROS [49]. The observation that H_2 treatment significantly improved the level of SH-SY5Y ATP and $\Delta\psi m$ in neuroblastoma [50] is an indication that H_2 treatment can elevate energy metabolism in mitochondria by activating oxidative phosphorylation. In conclusion,

H_2 can promote mitochondrial oxidative phosphorylation and maintain ROS dynamic balance to effectively protect the cell damage in the differentiation stage, and further promote the myogenic differentiation of stem cells. However, how mitochondrial function changes in the process of H_2-induced myogenic differentiation of stem cells remains to be studied.

As revealed from the mentioned results, H_2 could remarkably enhance ADSCs proliferation and myogenic differentiation, whereas the molecular system was unclear. Here, based on the p38 MAPK classes refer to signal transducing elements promoting myogenic differentiation in vitro and influencing muscle growing and repairing in vivo, whereas only p38 MAPK has a direct effect on myogenic transcribing elements of the Myod class [51, 52]. And through bioinformatics analysis infer H_2 was speculated to be involved in the p38 MAPK signaling pathway, probably affecting myogenic differentiation. During the differentiation, skeletal muscle cell can proliferate, migrate, subsequently seed from the cell cycle associated with an improvement in p38 MAPK signaling activity and then fuse to form multinucleated myotubes [53, 54]. To verify the probability of whether p38 signaling activity is required for myogenic differentiation induced by H_2, this study employed p38 MAPK kinase inhibitor (SB203580) capable of preventing the p38 to phosphorylation. As revealed from the results Western blotting assay, the H_2 can enhance p38 phosphorylating process, thereby improving the myogenic differentiation. When inhibitors (SB203580) were added, p38 and p-p38 expressions were significantly reduced. The results suggest that the H_2 can promote the myogenic differentiation through the stimulation of the p38 MAPK signaling pathway.

However, this study is limited as only in vitro experiments were performed. Future studies should therefore perform in vivo experiments to confirm these results.

5. Conclusion:

In brief, this study suggested that H_2 can promote myogenic differentiation via the p38 MAPK signaling pathways. H_2 also has a synergistic effect with 5-Aza to promote myogenic differentiation. Thus, the mentioned results are likely to elucidate myogenic differentiation and provide a high safety and efficacy alternative strategy for muscle damage and degeneration.

Abbreviations:

Full names	Abbreviations
5-Azacitidine	5-Aza
Adipose-derived Mesenchymal Stem Cells	ADSCs
Hydrogen	H_2
Myosin heavy chain	MHC
Volumetric muscle loss	VML

Declarations:

Ethics approval and consent to participate

All animal experiments were performed under the approval of the Institutional Animal Care and Use Committee of Jiangsu University.

Consent for publish

Not applicable.

Availability of data and materials

The data used and analyzed during the current study are available from the corresponding author on reasonable request.

Competing Interest

The authors declare that they have no competing interests.

Funding

This work was supported by the funds from the young medical key talent project of Jiangsu province (contract number QNRC2016458). Jiangsu Provincial Medical Innovation Team (Grant#CXTDB2017004).

Authors' contributions

Wenyong Fei, Erkai Pang and Jingcheng Wang: conception and design, financial support, experiment, manuscript writing, final approval of manuscript.

Erkai Pang made the equal contribution to the article and should be considered co-first author. Correspondence: Jingcheng Wang.

Lei Hou, Jihang Dai, Mingsheng Liu, Xuanqi Wang, Bin Xie,:analysis and interpretation of data and drafted the manuscript.

All authors read and approved the final manuscript.

References:

1. S.M. Abmayr, G.K. Pavlath, Myoblast fusion: lessons from flies and mice, Development. 139 (2012) 641–656. doi:10.1242/dev.068353.
2. S.M. Greising, G.L. Warren, W.M. Southern, A.S. Nichenko, A.E. Qualls, B.T. Corona, J.A. Call, Early rehabilitation for volumetric muscle loss injury augments endogenous regenerative aspects of muscle strength and oxidative capacity, BMC Musculoskelet. Disord. (2018) 1–11.

3. C.A. Aguilar, S.M. Greising, A. Watts, S.M. Goldman, J. Larouche, B.T. Corona, C. Peragallo, C. Zook, Multiscale analysis of a regenerative therapy for treatment of volumetric muscle loss injury, Cell Death Discov. (2018).
4. Valencia Mora M,Ruiz Ibán MA,Díaz Heredia J. Stem cell therapy in the management of shoulder rotator cuff disorders. World J Stem Cells 2015;7:691-699.
5. Hernigou P,Flouzat Lachaniette CH,Delambre J. Biologic augmentation of rotator cuff repair with mesenchymal stem cells during arthroscopy improves healing and prevents further tears:a case-controlled study. Int Orthop 2014;38□1811-1818.
6. J.M. Gimble, A.J. Katz, B.A. Bunnell, Adipose-derived stem cells for regenerativemedicine, Circ. Res. 100 (2007) 1249e1260.
7. B.E. Grottkau, Y. Lin, Osteogenesis of Adipose-Derived Stem Cells, Bone Res. 1 (2013) 133–145. doi:10.4248/BR201302003.
8. R. Dai, Z. Wang, R. Samanipour, K. Koo, K. Kim, Adipose-Derived Stem Cells for Tissue Engineering and Regenerative Medicine Applications, Stem Cells Int. 2016 (2016).
9. X. Xie, Y. Wang, C. Zhao, S. Guo, S. Liu, W. Jia, R.S. Tuan, C. Zhang, Comparative evaluation of MSCs from bone marrow and adipose tissue seeded in PRP-derived scaffold for cartilage regeneration, Biomaterials. 33 (2012) 7008–7018.
10. Y. Liu, X. Yan, Z. Sun, B. Chen, Q. Han, J. Li, R.C. Zhao, Flk-1+ Adipose-Derived Mesenchymal Stem Cells Differentiate into Skeletal Muscle Satellite Cells and Ameliorate Muscular Dystrophy in MDX Mice, Stem Cells Dev. 16 (2007) 695–706. doi:10.1089/scd.2006.0118.
11. A. Abdanipour, T. Tiraihi, A. Delshad, Trans-differentiation of the adipose tissue-derived stem cells into neuron-like cells expressing neurotrophins by selegiline, Iran. Biomed. J. 15 (2011) 113–121. doi:10.6091/ibj.1011.2012.
12. Mizuno, H. et al. Myogenic differentiation by human processed lipoaspirate cells. Plast. Reconstr. Surg. 109, 199e209; discussion 210-1(2002).
13. Michael J McClure, Koyal Garg, David G Simpson, John J Ryan, Scott A Sell, Gary L Bowlin, Jeffery J Ericksen. The influence of plate-rich plasma on myogenic differentiation. J Tissue Eng Regen Med 2016:10E239-E249.
14. Maria Maddalena Valente, Megan Allen, Valeria Bortolotto, Seung T Lim, Katherine Conant, Mariagrazia Grilli. The MMP-1/PAR-1 axis enhances proliferation and neuronal differentiation of adult hippocampal neural progenitor cells. Neural Plast, 2015.2015:p.646595
15. Zhao P, Jin Z, Chen Q, Yang T, Chen D, Meng J, LuX, Gu Z and HeQ: Local generation of hydrogen for enhanced photothermal therapy. Nat Commun 9: 4241, 2018.
16. Ohsawa I, Ishikawa M, Takahashi K, Watanabe M, Nishimaki K, Yamagata K, Katsura K, Katayama Y, Asoh S and Ohta S: Hydrogen acts as a therapeutic antioxidant by selectively reducing cytotoxic oxygen radicals. Nat Med 13: 688-694, 2007.

17. Ono H, Nishijima Y, Adachi N, Sakamoto M, Kudo Y, Nakazawa J, Kaneko K and Nakao A: Hydrogen(H_2) treatment for acute erythymatous skin diseases. A report of 4 patients with safety data and a non-controlled feasibility study with H2 concentration measurement on two volunteers. Med Gas Res 2: 14, 2012.
18. P. Guan, Z. M. Sun, L. F. Luo et al., “Hydrogen protects against chronic intermittent hypoxia induced renal dysfunction by promoting autophagy and alleviating apoptosis,” Life Sciences, vol. 225, pp. 46–54, 2019.
19. J. Li, Z. Hong, H. Liu et al., “Hydrogen-rich saline promotes the recovery of renal function after ischemia/reperfusion injury in rats via nti-apoptosis and anti-inflammation,” Frontiers in Pharmacology, vol. 7, p. 106, 2016.
20. N. Miyazaki, O. Yamaguchi, M. Nomiya, K. Aikawa, andJ. Kimura, “Preventive effect of hydrogen water on the development of detrusor overactivity in a rat model of bladder outlet obstruction,” The Journal of Urology, vol. 195, no. 3, pp. 780–787, 2016.
21. Y. Quan-Jun, H. Yan, H. Yong-Long, W. Li-Li, L. Jie, H. Jin-Lu, L. Jin, C. Peng-Guo,G.Run, G. Cheng, Selumetinib attenuates skeletal muscle wasting in murine cachexia model through ERK inhibition and AKT activation, Mol. Canc. Therapeut. 16(2) (2017) 334–343.
22. A. Suzuki, R. Minamide, J. Iwata, WNT/beta-catenin signaling plays a crucial role in myoblast fusion through regulation of nephrin expression during development,Development 145 (23) (2018).
23. S. Low, J.L. Barnes, P.S. Zammit, J.R. Beauchamp, Delta-like 4 activates Notch 3 to regulate self-renewal in skeletal muscle stem cells, Stem Cell. 36 (3) (2018)458-466.
24. A. Bohm, C. HoŤmann, M. Irmler, P. Schneeweiss, G. Schnauder, C. Sailer, V. Schmid, J. Hudemann, J. Machann, F. Schick, J. Beckers, M.H. de Angelis,H. Staiger, A. Fritsche, N. Stefan, A.M. Niess, H.U. Haring, C. Weigert, TGF-beta contributes to impaired exercise response by suppression of mitochondrial Key regulators in skeletal muscle, Diabetes 65 (10) (2016)2849-2861.
25. C.Q. Yi, D.D. Liu, C.C. Fong, J.C. Zhang, M.S. Yang, Gold nanoparticles promote osteogenic diŤerentiation of mesenchymal stem cells through p38 MAPK pathway, ACS Nano 4 (11) (2010) 6439–6448.
26. A.B. Lassar, The p38 MAPK family, a pushmi-pullyu of skeletal muscle diŤer-entiation, J. Cell Biol. 187 (7) (2009) 941–943.
27. Dr. Shigeyuki Wakitani; Dr. Tomoyuki Saito; Arnold I. Caplan (1995). Myogenic cells derived from rat bone marrow mesenchymal stem cells exposed to 5-azacytidine. 18(12), 1417–1426.
28. Yang, Mengling; Dong, Yinmiao; He, Qingnan; Zhu, Ping; Zhuang, Quan; Shen, Jie; Zhang, Xueyan; Zhao, Mingyi(2020). Hydrogen: A Novel Option in Human Disease Treatment. Oxidative Medicine and Cellular Longevity, (2020), 1–17.
29. Ohta S: Molecular hydrogen as a preventive and therapeutic medi-cal gas: initiation, development and potential of hydrogen medicine. Pharmacol Ther (2014) 144:1-11.
30. Ohsawa I, Ishikawa M, Takahashi K, Watanabe M, Nishimaki K, Yamagata K, Katsura K, Katayama Y, Asoh S and Ohta S:Hydrogen acts as a therapeutic antioxidant by selectively reducing cytotoxic

oxygen radicals. Nat Med (2007) 13:688-694.

31. Huang CS, Kawamura T, Toyoda Y and Nakao A: Recent advances in hydrogen research as a therapeutic medical gas. Free Radic Res (2010) 44:971-982.
32. Smith GCS,Bouwmeester TM,Lam PH.Knotless double-row SutureBridge rotator cuff repairs have improved self-reinforcement compared with double-row SutureBridge repairs with tied medial knots:a biomechanical study using an ovine model.J Shoulder Elbow Surg. 2017;26(12):2206-2212.
33. Kim KC,Shin HD,Cha SM. Comparisons of retear patterns for 3 arthroscopic rotator cuff repair methods. Am J Sports Med. 2014;42(3):558-565.
34. Megan L Killian,Leonardo M Cavinatto,Samuel R Ward,Necat Havlioglu,Stavros Thomopoulos,Leesa M Galatz.Chronic Degeneration Leads to Poor Healing of Repaired Massive Rotator Cuff Tears in Rats.Am J Sports Med. 2015;43(10):2401-2410.
35. Papa L, Djedaini M, Hoffman R. Mitochondrial role in stemness and differentiation of hematopoietic stem cells. Stem Cells Int. 2019;4067162.
36. Zhang H, Menzies KJ, Auwerx J. The role of mitochondria in stem cell fate and aging. Development. 2018;145(8):dev143420.
37. Ciciliot S, Schiaffino S. Regeneration of mammalianskeletal muscle. Basic mechanisms and clinical impli-cations. Curr Pharm Des. 2010;16(8):906–914.
38. Yu X, Zhang Y, Li T, et al. Long non-coding RNA Linc-RAM enhances myogenic differentiation by interact-ing with MyoD. Nat Commun. 2017;8(1):14016.
39. Paulin, D., & Li, Z. (2004). Desmin: A major intermediate filament proteinessential for the structural integrity and function of muscle.Experimental Cell Research,301,1–7.
40. K. Singh, F.J. Dilworth, DiŤerential modulation of cell cycle progression distinguishes members of the myogenic regulatory factor family of transcription factors, FEBS J. 280 (17) (2013) 3991–4003.
41. Yokoyama, S. & Asahara, H. 2011. The myogenic transcriptionalnetwork.Cell. Mol. Life Sci.68, 1843–1849.
42. E. Le Moal, V. Pialoux, G. Juban, C. Groussard, H. Zouhal, B. Chazaud, R. Mounier,Redox control of skeletal muscle regeneration, Antioxidants Redox Signal. 27(2017) 276–310.
43. L.L. Ji, C. Kang, Y. Zhang, Exercise-induced hormesis and skeletal muscle health,Free Radic. Biol. Med. 98 (2016) 113–122.
44. S.A. Mason, D. Morrison, G.K. McConell, G.D. Wadley, Muscle redox signallingpathways in exercise. Role of antioxidants, Free Radic. Biol. Med. 98 (2016) 29–45.
45. Michael C G,Anshuman S,Adam J E.The Role of Mechanobiology in Progression of Rotator Cuff Muscle Atrophy and Degeneration.J Orthop Res. 2018;6(2):546–556.
46. Oh JH,Chung SW,Kim SH.2013 Neer Award:Effect of the adipose-derived stem cell for the improvement of fatty degeneration and rotator cuff healing in rabbit model. J Shoulder Elbow Surg 2014;23(4):445-455.

47. Pas HIMFL, Moen MH, Haisma HJ. No evidence for the use of stem cell therapy for tendon disorders: a systematic review. Br J Sports Med. 2017;51:996-1002.
48. Osborne H,Anderson L, Burt P. Australasian College of Sports Physicians-position statement: the place of mesenchymal stem/stromal cell therapies in sport and exercise medicine. Br J Sports Med 2016;50:1237-1244.
49. SAITO T, SADOSHIMA J. The molecular mechanisms of mitochondrial autophagy /mitophagy in the heart. Circulation Research.2015;116(8):1477-1490.
50. Y. Murakami, M. Ito, and I. Ohsawa,"Molecular hydrogenprotects against oxidative stress-induced SH-SY5Y neuro-blastoma cell death through the process of mitohormesis,"PLoS One, vol. 12, no. 5, article e0176992, 2017.
51. R.L. Qi, H. Liu, Q. Wang, J. Wang, F.Y. Yang, D.B. Long, J.X. Huang, Expressionsand regulatory effects of P38/ERK/JNK mapks in the adipogenic trans-differentia-tionof C2C12 myoblasts, Cell. Physiol. Biochem. 44 (6) (2017) 2467–2475.
52. J.D. Bernet, J.D. Doles, J.K. Hall, K.K. Tanaka, T.A. Carter, B.B. Olwin, p38 MAPKsignaling underlies a cell-autonomous loss of stem cell self-renewal in skeletalmuscle of aged mice, Nat. Med. 20 (3) (2014) 265–271.
53. P. Brien, D. Pugazhendhi, S. Woodhouse, D. Oxley, J.M. Pell, p38 alpha MAPKregulates adult muscle stem cell fate by restricting progenitor proliferation duringpostnatal growth and repair, Stem Cell. 31 (8) (2013) 1597–1610.
54. A. Cuenda, J.J. Sanz-Ezquerro, p38 gamma and p38 delta: from Spectators to KeyPhysiological Players, Trends Biochem. Sci. 42 (6) (2017) 431–442.

Table:

Table 1 is not available with this version.

Figures

Figure 1

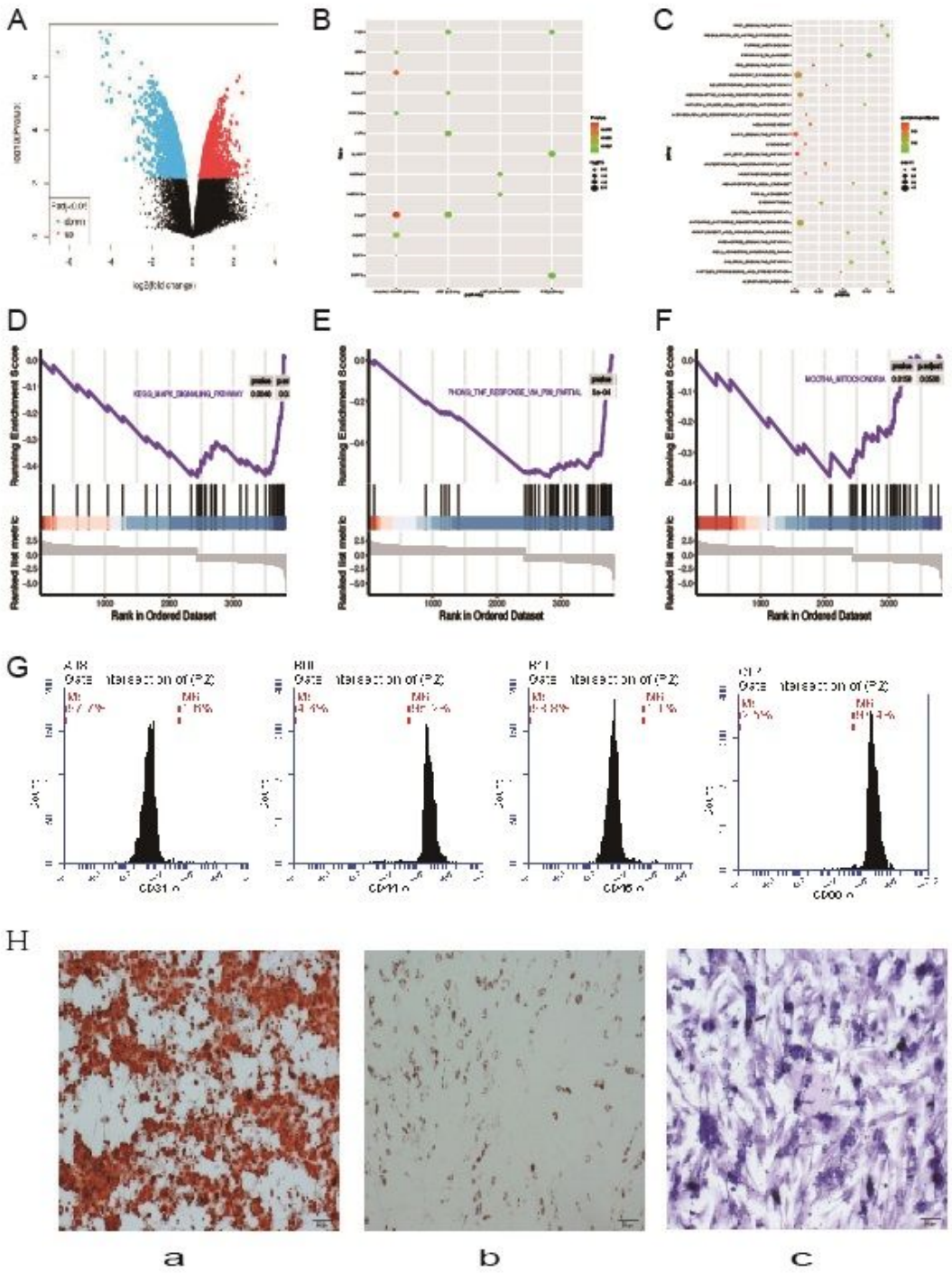

Figure 1

Figure1(A)Volcanic map of cells cultured in hydrogen shows differentially expressed genes; (B)KEGG enrichment pathway analysis; (C)Analysis of differential gene expression in MAPK signaling pathway, GSEA enrichment analysis; (D)Enrichment analysis of MAPK signal pathway; (E)Enrichment analysis of p38-MAPK signal pathway; (F)Mitochondrial functional enrichment analysis; Figure1(G-H). Identifification of adipose-derived stem cells (ADSCs). Figure1(G). Flow cytometry analysis results and expression of cell

surface CD markers of ADSCs at passage 3. The x-axis is the fluorescence intensity, and the y-axis is the cell number; Figure1(H). ADSCs was positive for Alizarin red (a), Oil Red O (b), and Toluidine blue staining (c) after induced differentiation.

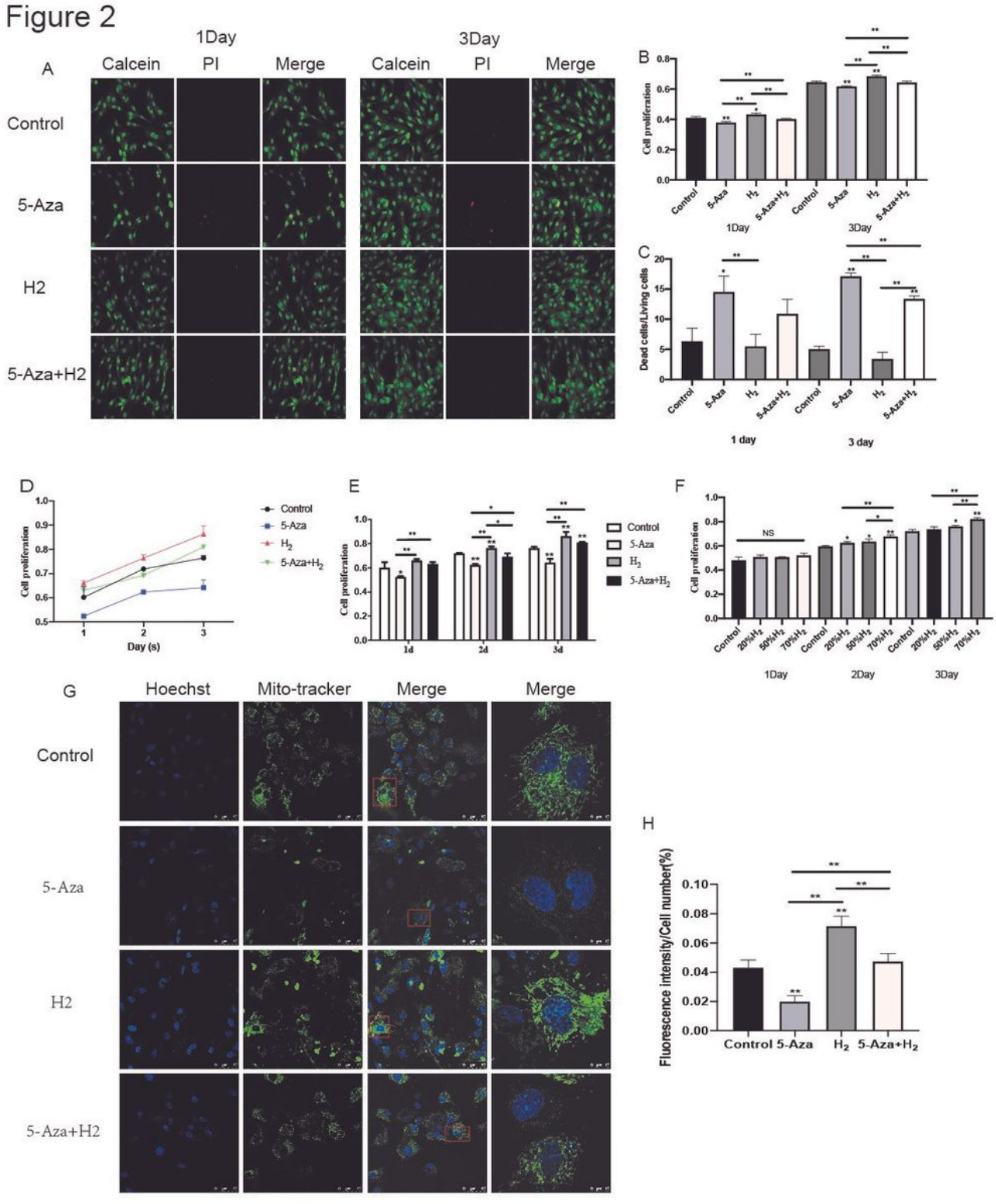

Figure 2

Figure(2A-C). ADSCs viability evaluation after cultured with different differentiation medium for 1 to 3 days. (A) Live-Dead cell staining analysis and Alamar blue staining on 1 and 3 days; (B) Fluorescence

quantitative analysis of cell proliferation; (C) Proportion analysis of live-dead cells. Figure(2D, E). Cell viability was assessed by MTT. Figure(2F). Selection of the optimum concentration of hydrogen. Figure(2G, H). The analysis of mitochondrial staining. (G) Fluorescent staining of mitochondria by Mito-tracker; (H) Quantitative analysis of fluorescence intensity of single cell mitochondria. All experiments were performed in triplicate (*p< 0.05, **p< 0.01).

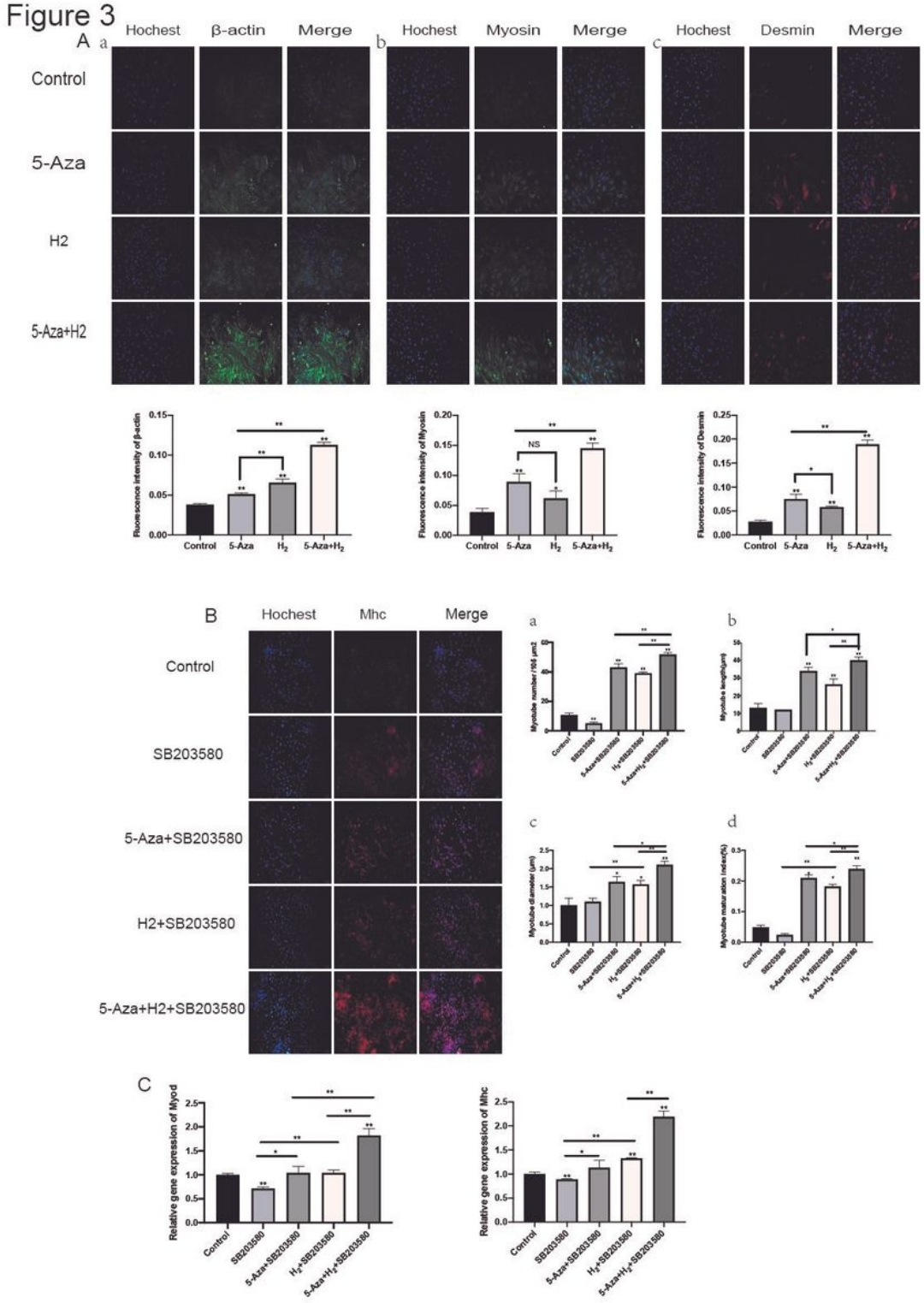

Figure 3

Figure 3A. β-actin, Myosin and Desmin expression (Immunofluorescence staining). Molecular expression levels of a) β-actin, b) Myosin and c) Desmin; Figure 3B. Observation and analysis of myotube. Immunofluorescence staining of Mhc protein (red) in ADSCs on day 7 in myogenic differentiation medium; Quantitative analysis of myotube number (a), myotube length (b), myotube diameter (c), and myotube maturation index (myotubes with≥2nuclei) (d); Figure 3C. Myod and Mhc expression (RT-PCR). All experiments were performed in triplicate (*p< 0.05, **p< 0.01).

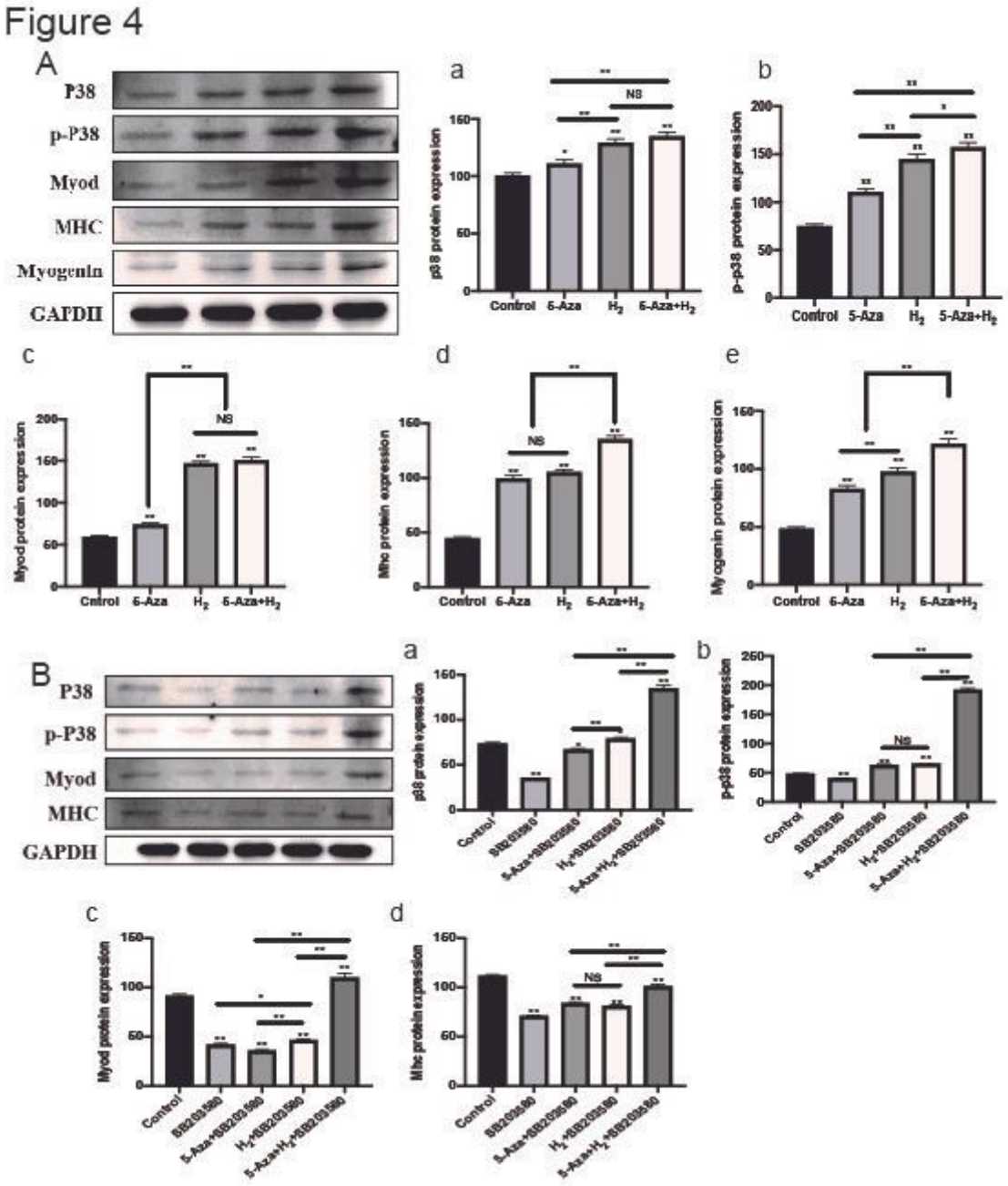

Figure 4

Figure 4A. Myod, Mhc, Myogenin, p38 and p-p38 expression (Western blot). Figure 4B. Molecular mechanism analysis of myogenic differentiation. (B)Western blot analysis of p38 MAPK pathway related proteins in ADSCs on day 7 after incubation with inductor in inhibitor added myogenic differentiation

medium; Quantitative gray level based on the Western blot bands for P-p38, p38, Mhc and Myod proteins expression; All experiments were performed in triplicate (*p< 0.05, **p< 0.01).